Indian Journal of Chemical Technology
Vol. 32, November 2025, pp. 697-709
DOI: 10.56042/ijct.v32i6.22215

Utilizing tea waste for methylene blue removal: Insights from batch and fixed-bed adsorption studies

Saurabh Meshram[1], Nikhil Rahul Dhongde[2]*, Shivani Suryavanshi[1], Amit Chaudhary[1] & Dhanjit Rajbongshi[1]
[1]Department of Chemical Engineering, Guru Ghasidas Vishwavidyalaya Bilaspur, Chhattisgarh 495 009, India
[2]Department of Chemistry, University of Saskatchewan, Saskatoon, Saskatchewan, S7N 5C9, Canada
*E-mail: nikhildhongde9194@gmail.com / nikhil.rahul@usask.ac

Received 31 July 2025; accepted 13 October 2025

This study explores the potential of tea waste as a cost-effective and eco-friendly biosorbent for the removal of hazardous methylene blue (MB) dye from aqueous solutions. The tea waste-based adsorbent has been synthesised and characterised using Fourier transform infrared spectroscopy, X-ray diffraction, and scanning electron microscopy to examine its functional groups, crystallinity, and surface morphology. Batch adsorption experiments evaluated the impact of initial dye concentration, contact time, and adsorbent dosage. Isotherm analysis revealed Langmuir model compatibility with a high monolayer capacity (q_{max} = 454.54 mg/g), indicating effective surface interaction. Kinetic modeling showed excellent fit with the pseudo-second-order model ($R^2 = 1.000$), suggesting chemisorption as the primary mechanism. A fixed-bed column study assessed the effects of flow rate, bed height, and column diameter on breakthrough behaviour. Optimal conditions 4 mL/min flow rate, 2 cm bed height, and 1.5 cm column diameter achieved a 105 min. breakthrough time. Process optimization via Box–Behnken response surface methodology confirmed the model's predictive strength. The results demonstrate that tea waste is a promising low-cost biosorbent for the efficient removal of MB dye, with potential application in wastewater treatment systems.

Keywords: Adsorption, Column Adsorption, Dyes, Methylene Blue, Tea waste, Wastewater

Introduction

Tea, derived from the tender leaves of *Camellia sinensis*, is one of the most consumed beverages globally, second only to water. With a global consumption of 5.8 million tons in 2019, rising to 6.3 million tons in 2020, and projected to hit 7.5 million tons by 2025, its popularity shows no sign of slowing[1]. Major producers include China (2.74 million tons), India (1.33 milliontons), Sri Lanka (0.278 million tons), and Kenya (0.569 million tons). However, this booming industry generates significant biomass waste from unplucked leaves and pruned branches to spent tea leaves (STLS), which make up nearly 90% of the solid residue after tea extraction[2,3]. Waste is further amplified by widespread consumption in households, restaurants, and hotels. This not only strains waste management systems but also impacts the environment[4,5]. Harnessing tea waste for sustainable applications is crucial to turning this challenge into an opportunity for environmental and economic benefits[6–10]. Hussain *et al.*[11] stated that waste tea material possesses the potential to serve as low-cost adsorbents for various metal ions and other wastewater effluents.

As of 2025, methylene blue (MB) dye continues to present serious environmental and health concerns due to its widespread industrial use. Annually, more than 10,000 tonnes of MB are utilised worldwide in textiles, medicines, and aquaculture, with a substantial amount released into aquatic environments without sufficient treatment[12–14]. Research indicates that MB concentrations in untreated textile effluents can attain levels of up to 150 mg/L, far beyond acceptable environmental limits (<1 mg/L). In aquatic habitats, MB diminishes light penetration by as much as 60%, obstructing photosynthesis and decreasing dissolved oxygen levels, perhaps resulting in a 40–70% reduction in microbial activity[15–18]. Exposure to MB concentrations over 20 mg/kg in humans may lead to symptoms including cyanosis, haemolytic anaemia, and potentially lethal consequences in those with glucose-6-phosphate dehydrogenase deficiency.

Adsorption is widely used due to its affordability, simplicity, efficiency, fast results, minimal by products, and biocompatibility. A notable type is biosorption, which uses biologically derived sorbents. Wastewater treatment poses significant challenges, as traditional approaches such as activated carbon adsorption attain about 70–80% effectiveness, but innovative photocatalytic systems utilising nanomaterials have exhibited degradation rates over 90-94 % in laboratory conditions[19]. In recent years, various types of adsorbents have been employed for the absorptive removal of MB from aqueous solutions[20–29]. Nonetheless, cost and scalability continue to pose challenges.

A multitude of studies have been undertaken in recent years to eradicate MB by utilising tea waste as an adsorbent, such as Uddin *et al.*[30] demonstrated that tea waste is an effective, low-cost adsorbent for removing MB from water. Batch studies confirmed its strong adsorption capacity through kinetic and isotherm analyses. Ullah *et al.*[31] recorded the kinetic studies for three different temperatures, i.e., 293 K, 303 K, and 313 K. El-Azazy *et al.*[32] synthesise adsorbent via thermal treatment (250–500°C) of raw green tea waste and used for MB removal.

Most adsorption studies involving MB dye and tea waste as an adsorbent have primarily been conducted using batch systems. While suitable for controlled laboratory investigations, batch methods are generally impractical for large-scale or continuous flow applications. These systems are mainly used to estimate the maximum adsorption capacity and assess the effectiveness of the adsorbent in removing specific contaminants under static conditions. However, for real-world or industrial-scale wastewater treatment, continuous systems are more appropriate. Fixed-bed column adsorption offers a practical alternative, allowing for continuous flow treatment and the acquisition of essential operational data such as bed exhaustion time, breakthrough behaviour, and regeneration intervals. The breakthrough curve generated from column experiments provides insights into the dynamic performance of the adsorbent. Using a fixed-bed column with tea waste to remove MB dye not only demonstrates the feasibility of continuous operation but also offers advantages such as ease of integration into existing processes, reduced chemical usage, and lower operational costs, making it well-suited for large-scale wastewater treatment systems.

Although batch adsorption studies have investigated the removal of MB dye using tea waste[30], they have predominantly focused on batch systems. To date, no research has explored both batch and continuous adsorption using unmodified tea waste as the adsorbent for MB dye removal, highlighting a clear gap in the literature. In this study, the adsorption performance was evaluated in both systems, and a mechanism for MB dye removal using tea waste was proposed based on the observed results. Furthermore, non-destructive techniques such as FTIR, XRD and SEM were employed before and after adsorption to gain insights into the adsorption mechanism. Finally, the results of this work enhance the sustainability and practical applicability of tea waste-based adsorption in wastewater treatment. These adsorbents show strong potential for use in decentralized water treatment systems, particularly in rural or resource-limited settings, and contribute valuable insights for scaling up to full-scale treatment plants.

Experimental Section

Materials & reagents

Tea waste adsorbent

Used tea leaves were collected from a local tea shop located near Guru Ghasidas Vishwavidyalaya, Bilaspur, Chhattisgarh, India. The collected tea waste was initially subjected to thorough washing with distilled water to eliminate dust, soluble impurities, and residual sugar or milk content. After washing, the tea waste was dried in a hot air oven (P S Instruments Private Limited, Gujarat, India) at a controlled temperature of 60±2 °C for a duration of 24 h to reduce the moisture content to below 5±2 %. Once adequately dried, the tea waste was ground using a mechanical grinder and sieved to obtain a powder with a particle size of 100 mesh. The finely powdered tea waste was then stored in a clean, airtight container to prevent moisture absorption and contamination prior to its use in adsorption experiments.

Methylene blue solution

A stock solution of MB dye was prepared by dissolving 1.0 g of analytical grade MB in 1 L of distilled water. The solution was stirred thoroughly to ensure complete dissolution and stored in a dark, airtight container at room temperature to prevent degradation. The concentration of MB was confirmed using a UV-visible spectrophotometer by measuring the absorbance at 660 nm.

Batch adsorption experiments

Batch experiments were conducted to assess the adsorption process under different parameters, where the process of initial dye concentration was examined. In these experiments, dye concentration was varied as 50 ppm, 100 ppm, 150 ppm and 200 ppm. The amount of the adsorbent added was 0.5 g in a 100 mL conical flask, and agitated for 90 min in an orbital incubator. For the adsorbent dosage study, the concentration of dye solution was kept constant at 150 ppm in a conical flask and the dosage were altered as 0.1 g, 0.3 g, 0.5 g and 0.7 g and agitated for same interval of time of 90 min. In the study of contact time, the concentration and dosage were kept constant at 150 ppm and 0.5 g, respectively. The agitation time was altered as (60, 120, 180, 240 min).

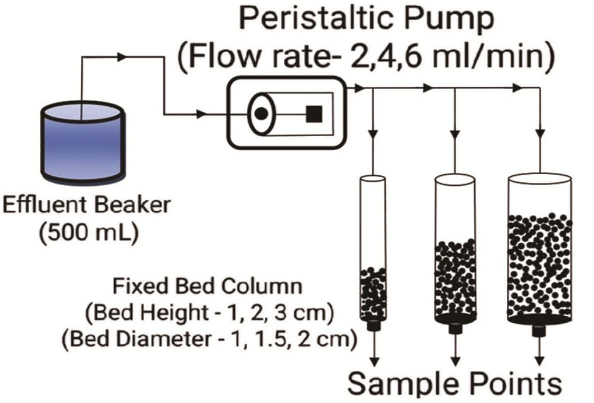

Fig. 1 — Schematic diagram of the continuous adsorption experimental setup

Continuous adsorption experiment

The continuous experiment was performed to study the adsorption of MB dye from aqueous solutions using tea waste as a low-cost adsorbent in a fixed-bed column. The continuous adsorption experiment setup is presented in Fig. 1. The Box-Behnken design is useful for minimizing extreme experimental conditions, as it prevents all factors from being at their maximum or minimum values simultaneously[33]. It is particularly effective when dealing with three levels of factors, which makes it an ideal choice for this experiment. This approach utilises Eq. (1) to ascertain the quantity of experiments.

$$N = 2k\,(k-1) + \theta o \qquad \ldots (1)$$

Where N is the number of experiments, k is the factor, and θo is the replicate number of the central point. The effect of process parameters on continuous adsorption was studied using response surface methodology based on Box-Behnken experimental design for the three factors at three levels using Minitab Statistical Software 22[34]. Table 1 represents the factors and their level for this design of the experiment. The actual design matrix for the experiments is given in Table 2. A total of 15 runs of experiments according to the matrix were performed for the optimisation of parameters. According to the

Table 1 — Parameters and corresponding values for the Box-Behnken Design experiment in fixed bed adsorption

Code	Parameter	Unit	Min value	Max value	Mean value
A	Flow rate	mL/min	2.0	6.0	4.0
B	Bed height	cm	1.0	3.0	2.0
C	Bed diameter	cm	1.0	2.0	1.5

Table 2 — Various Parameters by Box-Behnken Design for continuous adsorption experiment

Run	Flow Rate (mL/min)	Bed Height (cm)	Bed Diameter (cm)	Breakthrough Time (min)
1	4	2	1.5	105
2	4	1	2	67
3	2	2	1	77
4	4	1	1	55
5	6	2	2	66
6	6	3	1.5	80
7	6	1	1.5	45
8	4	3	1	60
9	4	3	2	62
10	2	3	1.5	99
11	6	2	1	15
12	4	2	1.5	103
13	2	1	1.5	50
14	4	2	1.5	108
15	2	2	2	89

Box-Behnken experimental design, the effect of flow rate (2, 4, and 6 mL/min), adsorbent bed diameter (1.0, 1.5, and 2.0 cm), and adsorbent bed depth (1, 2, and 3 cm) on breakthrough time was determined.

Experimental work

To conduct the trial effectively, a custom-designed yet straightforward inflow system was developed. Central to this setup was a saline bottle, which served as the force for the MB colour result and worked as the effluent vessel throughout the study. A saline tube was connected to the outlet of the bottle to transport the MB dye to the adsorption column. At the terminal end of this tube, an injection needle was attached. This needle acted as a physical inflow restrictor due to its narrow drag, offering fresh subcaste of control over the liquid's discharge rate. Each trial began with the saline bottle being filled with 500 mL of MB dye. The experimental design was structured around three crucial process parameters: flow rate, adsorbent bed height, and bed diameter. These parameters were totally varied following the principles of the Box-Behnken Design, a type of response surface methodology used to optimise conditions while minimising the number of experimental runs[35,36]. To acclimate and maintain the required inflow rate, a comber clamp was installed along the saline tube. This simple mechanical device allowed for precise homemade control of the inflow. Rolling the clamp overhead increased the inner tube periphery and therefore the inflow; while rolling it down confined the inflow. For each run, the inflow rate was calibrated using a stopwatch and a measuring cylinder. A given volume of results was collected over time. During each trial, liquid samples were collected at regular intervals and analyzed for the concentration of MB dye.

Characterisation

The functional group and chemical structure of the tea waste adsorbent before and after adsorption were determined through an FTIR (Shimadzu IR affinity-1) and X-ray diffraction (9 kW powder XRD, Rigaku Technologies, Smart lab). The morphologies of the tea waste adsorbent before and after adsorption were studied using scanning electron microscope (SEM) (Zeiss, Sigma 300).

Results and Discussion

Characterisation of tea waste adsorbent

SEM analysis

Fig. 2 shows an SEM micrographs of the tea waste adsorbent before and after adsorption at 50 and 5 μm magnification. In general, the adsorbent exhibits a heterogeneous or rough and porous (caves) surface structure, which is favourable for the adsorption of MB dye[37]. As observed in Fig. 2 (SEM before

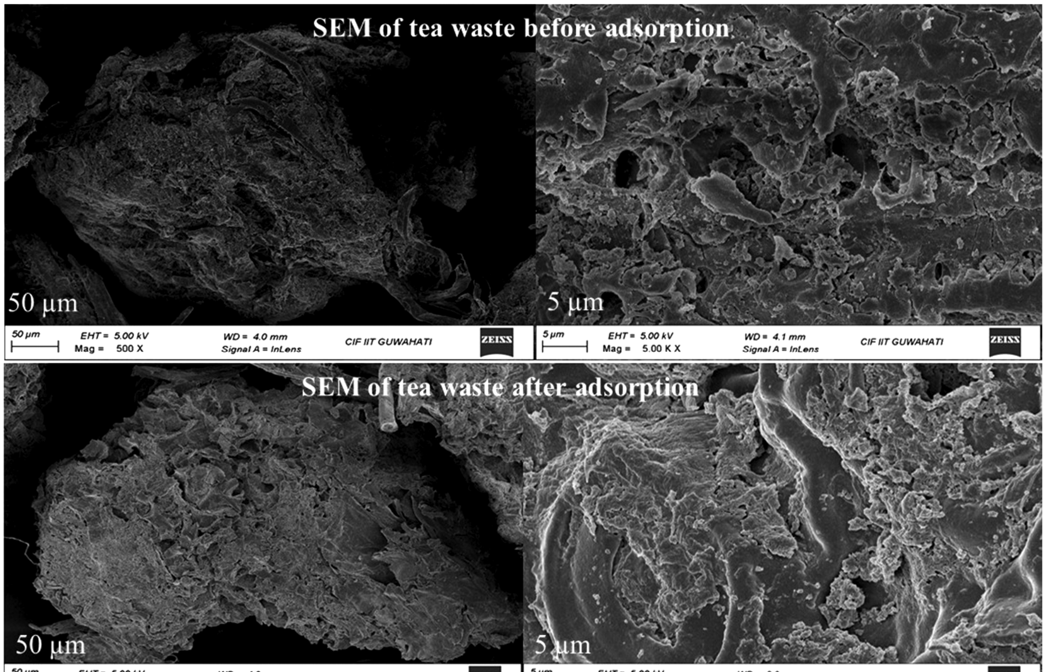

Fig. 2 — SEM image of tea waste adsorbent before (upper panel) and after adsorption (lower panel)

absorption), the tea waste adsorbent presented a stem structure on the surface due to its main components, including cellulose and hemicellulose[38]. Additionally, the SEM images of the tea waste adsorbent suggested a rough, uneven surface with pores, which presents a likely large surface area with many active sites for adsorption applications.

Post-adsorption, the surface of the tea waste appeared significantly smoother, with many surface pores visibly filled or blocked by MB dye molecules, suggesting that adsorption occurred both on the external surface and within the internal pore structure. This reduction in surface roughness and porosity confirms the presence of MB on the adsorbent. The physical adsorption mechanism is supported by these observations, likely driven by surface-level interactions between the cationic MB molecules and negatively charged functional groups, primarily hydroxyl (–OH) and carboxyl (–COOH) on the tea waste surface[39–41]. These morphological changes provide strong visual evidence for the efficacy of tea waste adsorbent as a low-cost, sustainable adsorbent for the removal of MB from aqueous solutions. Similar patterns were seen in the SEM images of tea waste adsorbents used for dye removal, as reported by Hussain *et al.*[11] and Uddin *et al* [30].

FTIR analysis

The FTIR spectra of the tea waste adsorbent before and after MB adsorption (Fig. 3) reveal key functional group interactions. A broad peak around 3414.90 cm^{-1} before adsorption, shifting slightly to 3422.94 cm^{-1} after, corresponds to O–H stretching vibrations of hydroxyl groups in cellulose, lignin, and hemicellulose, indicating their involvement in adsorption[42]. The peak at 2921.53 cm^{-1} is attributed to aliphatic C–H stretching, while a shoulder at 1651.78 cm^{-1} suggests C=O stretching, likely from lignin components[43]. A strong band at 1062.20 cm^{-1} represents C–O–H stretching, and the peak at 1449 cm^{-1} is associated with NH_2 or C–H bending. Shifts and changes in these bands after adsorption confirm the interaction between MB molecules and active functional groups on the tea waste surface. The shift of the peak from 1449 cm^{-1} to 1402 cm^{-1} after adsorption indicates the involvement of –COOH (carboxyl) groups in the binding process[42,44]. This shift suggests that the carboxyl groups participated in interactions with the MB dye molecules. Additionally, the observed changes in peak positions confirm that electrostatic attractions occurred between the cationic MB dye and negatively charged functional groups such as –OH and –NH_2 present on the tea waste biosorbent[45,46]. These interactions play a key role in the adsorption mechanism, facilitating the attachment of MB dye molecules to the tea waste adsorbent surface. Prior studies demonstrated that analogous functional groups facilitate the adsorption process[47–50].

XRD analysis

In the XRD pattern (Fig. 4) of the raw tea waste, a prominent peak at 21.8° corresponds to the (002) crystalline plane of cellulose, while two shoulder peaks at approximately 15° and 16.5° are attributed to the presence of lignin and hemicellulose, respectively[51,52]. The overall pattern exhibited broad and low-intensity peaks, characteristic of an amorphous structure, which is typical of lignocellulosic biomass due to the lack of long-range crystalline order in cellulose, hemicellulose, and lignin[53]. After MB adsorption, the

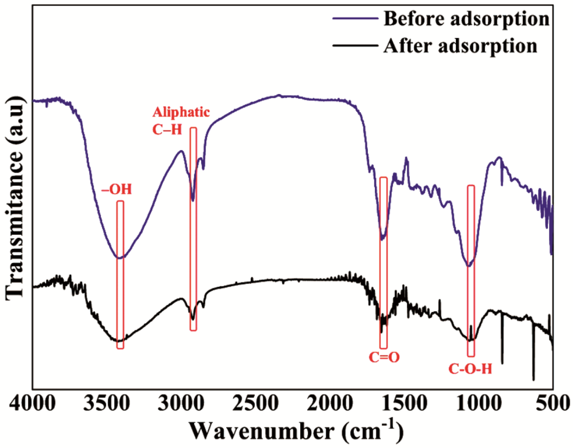

Fig. 3 — FTIR spectra of tea waste adsorbent before and after adsorption

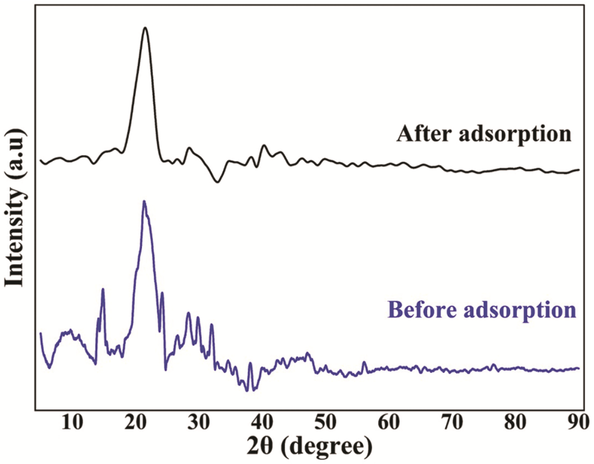

Fig. 4 — XRD plot before and after adsorption of MB dye onto tea waste

shoulders corresponding to lignin and hemicellulose disappeared, while the cellulose peak at 21.8° remained, suggesting that MB molecules interacted predominantly with the amorphous regions of the tea waste matrix. No new crystalline peaks were observed in the XRD pattern post-adsorption, indicating that the adsorption process did not induce any significant structural reordering or crystallinity within the material. These observations confirm that tea waste retains its amorphous nature after MB adsorption, and the interaction mechanism is likely governed by physical adsorption, involving van der Waals forces, hydrogen bonding, or electrostatic attractions between the dye molecules and the functional groups on the tea waste surface [54,55].

The combined results from SEM, FTIR, and XRD analyses confirm that tea waste possesses the capability to adsorb dye molecules, with clear evidence of MB adsorption onto the surface and within the structure of the adsorbent. Morphological changes, functional group interactions, and the preservation of the amorphous structure all support the occurrence of physical adsorption.

Batch adsorption study

Effect of contact time on MB dye removal

Based on preliminary batch experiments conducted in our laboratory, the influence of contact time on the adsorption efficiency was evaluated using a fixed mass (0.5 g) of tea waste as the adsorbent and 100 mL of MB solution at an initial concentration of 150 ppm. The temporal adsorption profile of MB onto tea waste is illustrated in Fig. 5a. The results demonstrate that the extent of adsorption increases with prolonged contact time. The adsorption process exhibited an initial rapid uptake phase, attributed to the abundance of available active sites on the tea waste surface and a steep concentration gradient between the bulk solution and the adsorbent interface. As adsorption progressed, the number of accessible active sites diminished, and the concentration gradient decreased, resulting in a reduced adsorption rate over time. This deceleration suggests the approach toward equilibrium. Identifying the optimal contact time is essential for optimising process design and ensuring the cost-effective removal of MB dye from aqueous systems.

Effect of initial MB dye concentration

The plot of the effect of initial MB dye concentration on the removal of MB dye is presented in Fig. 5b. It shows that the removal efficiency decreased with the increase in initial concentrations, although the amount of total MB dye accumulation increased. The total accumulation of MB dye increased with increasing initial concentration was probably due to more contact of adsorbent sites with MB dye. At higher initial concentrations of MB dye, the driving force for the adsorption process increases. This means that more MB dye molecules are available in the solution to interact with the adsorbent (tea waste), leading to a faster adsorption rate initially. With a higher initial MB dye concentration, the time required to reach adsorption equilibrium may decrease because the adsorbent is initially more saturated with MB dye molecules, which accelerates the adsorption process.

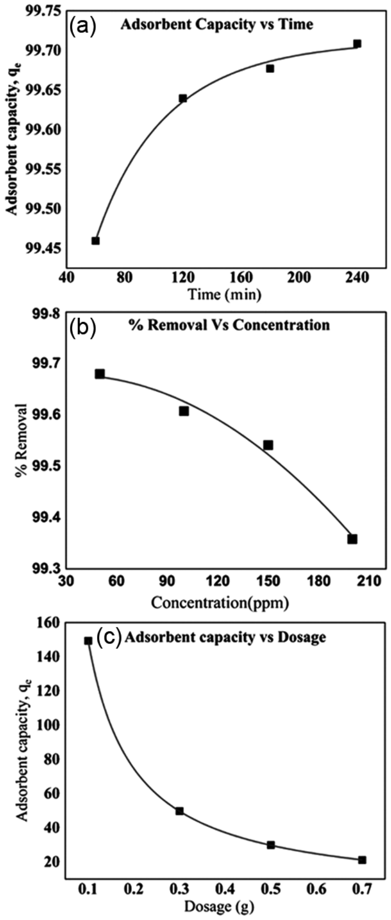

Fig. 5 — (a) Effect of contact time on the adsorption of MB dye onto tea waste (60, 120, 180, 240 min. in 150 ppm of MB dye solutions), (b) effect of initial MB dye concentration on the removal of MB dye (time-90 min, in 50, 100, 150, 200 ppm of MB dye solutions of 0.5 g of adsorbent), and (c) plot of effect of adsorbent dosage on the adsorption of MB onto tea waste (time-90 min, of 0.1, 0.3, 0.5, 0.7 g. of adsorbents, in 150 ppm of MB dye solution)

Effect of tea waste adsorbent dosage

The plot of the Effect of adsorbent dosage on the adsorption of MB onto tea waste is presented in Fig. 5c. Initially, increasing the amount of adsorbent usually increases the adsorption capacity because more surface area becomes available for adsorbate molecules. This can lead to a higher quantity of the target substance (adsorbate) being adsorbed. Increasing the adsorbent dosage generally speeds up the rate of adsorption, as more adsorbent sites are available for interaction with the adsorbate. This could lead to a more rapid removal of the adsorbate from the solution, particularly during the initial stages of the process. After a certain dosage, the adsorption capacity tends to plateau. This happens because the adsorbent sites become saturated. In other words, the adsorbent reaches a point where there are no more vacant sites for the adsorbate to bind to, and increasing the dosage further will have little effect.

Isotherm study

Langmuir and Freundlich isotherm models were used to determine the mechanism of adsorption of MB dye onto tea waste adsorbent. The analysis and design of the adsorption process require the relevant adsorption equilibria to better understand the adsorption process[56,57]. Adsorption equilibrium provides fundamental physicochemical data for evaluating the applicability of the sorption process as a unit operation[57,58]. In the present investigation, the equilibrium data were analyzed using Langmuir and Freundlich isotherm expressions given by the following equations, respectively,

$$\text{Langmuir: } \frac{1}{q_e} = \frac{1}{K_L\, q_{max}} \cdot \frac{1}{C_e} + \frac{1}{q_{max}} \qquad \dots (2)$$

$$\text{Freundlich: } Logq_e = LoqK_f + \frac{1}{n}\, LogC_e \qquad \dots (3)$$

Where, K_f and n are Freundlich constants related to sorption capacity and sorption intensity of adsorbents. The value of n falling in the range of 1–10 indicates favourable adsorption. q_e is the adsorption density at equilibrium of MB, Ce is the equilibrium concentration of the dye in solution, q_0 is the monolayer adsorption capacity, and K_L is the Langmuir constant related to the free energy of adsorption.

Fig. 6(a–b) presents the adsorption equilibrium data fitted to Langmuir and Freundlich isotherm models, represented by Eqs (1) and (2), respectively. The experimental data of Langmuir and Freundlich isotherm models for the adsorption of MB dye onto tea waste adsorbent are presented in Table 3. The comparative analysis of the fitting indicates that Langmuir model provides a significantly better correlation with the experimental data than Freundlich model, suggesting monolayer adsorption behaviour of MB onto the surface of tea waste. All the models exhibited very high R² values. The RMSE values for the Langmuir and the Freundlich isotherms were 0.0010 and 0.0096, respectively. The Langmuir constant, K_L=0.01 (L/mg), reflects a high affinity between the adsorbent and adsorbate, indicating a much faster adsorption rate relative to desorption. In contrast, the Freundlich constants, K_f=10.01 (mg/g) $(L/mg)^{1/n}$ and n=0.97, imply a moderately favourable adsorption process with heterogeneous surface characteristics, though with less predictive power than the Langmuir model. The maximum monolayer adsorption capacity q_{max} derived from the Langmuir model was found to be 454.54 mg/g. The isotherms outcomes suggest that the adsorbent surface is

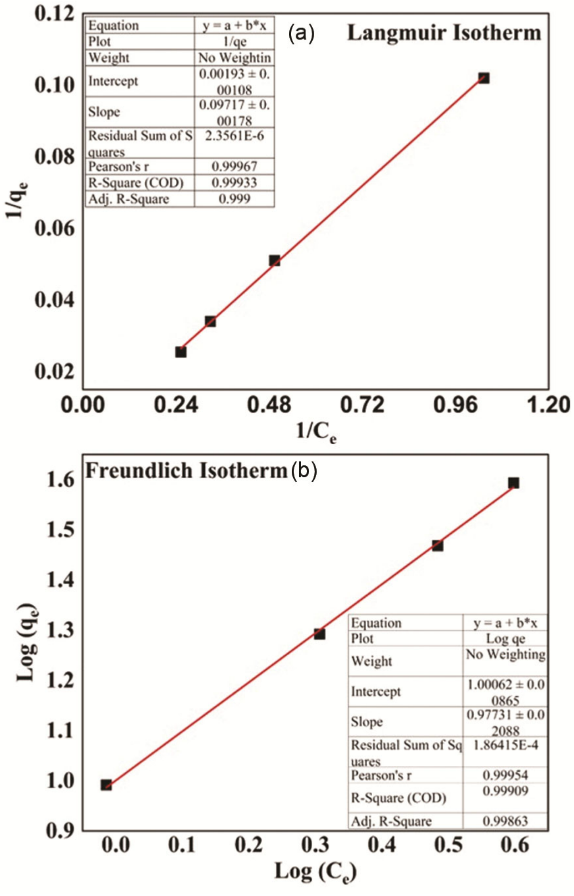

Fig. 6 — Linear fit of (a)Langmuir and (b) Freundlich isotherm model for the adsorption of MB

Table 3 — Experimental data of the isotherm model for the adsorption of MB dye onto tea waste

Langmuir	q_{max}(mg/g)	K_L	R_L	R^2	RMSE
	454.54	0.01986	0.5017	0.9993	0.0010
Freundlich	1/n	K_f	R^2		RMSE
	0.97	10.01	0.9990		0.0096

Table 4 — Kinetic model parameters

	First-order kinetic model			Second-order kinetic model	
q_e(mg/g)	K_1 (1/min)	R^2	q_e(mg/g)	K_2 (g/mg/min)	R^2
1.320	0.005	0.957	29.949	0.147	1.00

somewhat heterogeneous, and the adsorption process is mainly governed by physicochemical interactions.

Adsorption kinetic models

To investigate the adsorption mechanism, batch adsorption data are fitted to different kinetic models. The pseudo-first-order and pseudo-second-order models are commonly used to assess the kinetics of the process. The estimated parameters for these models are summarized in Table 4.

Pseudo-first-order model

This model assumes that the adsorption of metal ions is directly related to the availability of active sites on the adsorbent surface and is represented by Eq. (4) [59,60].

$$log(q_e - q_t) = log\, q_{e\,cal} - \frac{k_1}{2.030}t \quad \ldots (4)$$

Where k_1 represents the first-order rate constant (min^{-1}), $q_e$is the adsorbent uptake capacity at the equilibrium, and qt is the adsorbent uptake capacity at time *t*.

By plotting ln(q_e-q_t) versus time (t), the values of k_1 and q_e can be estimated. However, the pseudo-first-order model yielded low correlation coefficients, and there were significant discrepancies between the experimental and calculated equilibrium adsorption capacities (q_e). These findings suggest that this model does not effectively describe the experimental data.

Pseudo-second-order model

In this approach, the adsorption rate is considered to be proportional to the square of the difference between the amount of adsorbate at equilibrium and that at a given time t, as described by the published literature [61]. The model is often represented in its linearized form, as shown in Eq. (5).

$$\frac{t}{q_t} = \frac{1}{K_2 q_e^2} + \frac{t}{q_e} \quad \ldots (5)$$

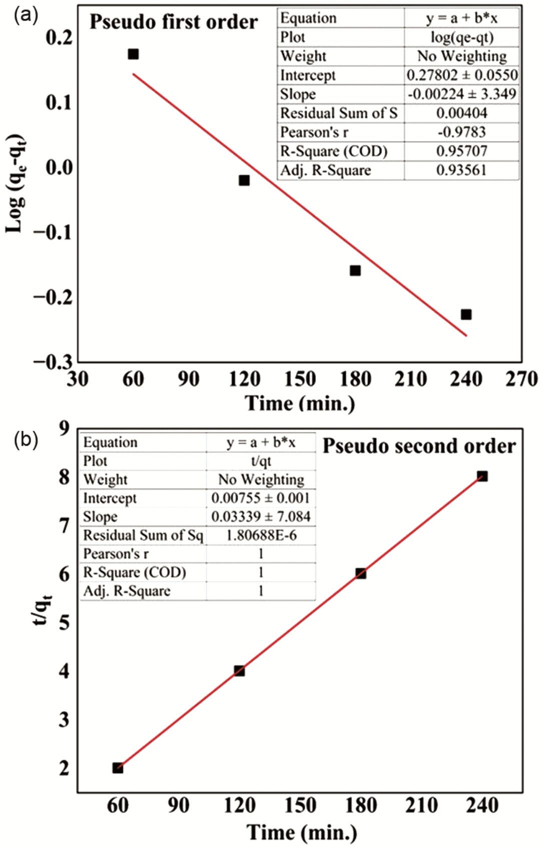

Fig. 7 — Plot of (a) pseudo first order (b) pseudo second order kinetics for adsorption of MB dye onto tea waste adsorbent

Where, the equilibrium rate constant for pseudo-second-order adsorption is denoted by K_2 (g/mg min). By plotting t/q_t against time (t), a linear relationship is obtained (Fig. 7), and the slope and intercept of this line are utilized to compute the values of q_e and K_2. The kinetic modelling of MB dye adsorption onto tea waste was evaluated using both pseudo-first-order and pseudo-second-order kinetic models.

The experimental data exhibited a significantly better fit to the pseudo-second-order model, as evidenced by a correlation coefficient (R^2) of 1.000, in contrast to the pseudo-first-order model, which yielded an R^2 value of 0.957. This superior fit indicates that the adsorption process follows a pseudo-second-order kinetic mechanism, implying that the rate-limiting step may involve chemisorption, characterised by valence forces through the sharing or exchange of electrons between the adsorbent and adsorbate. The adsorption behaviour suggests a heterogeneous surface interaction wherein the process initiates with physisorption, driven by weak van der Waals forces, and progressively transitions into chemisorption as active functional groups on the tea waste surface interact more strongly with MB dye molecules. This sequential adsorption mechanism is further corroborated by FTIR spectroscopic analysis (Fig. 3), which reveals significant changes in the vibrational frequencies of functional groups such as hydroxyl (–OH), aliphatic C–H, and other oxygen-containing groups before and after adsorption. The observed spectral shifts confirm the involvement of these functional groups in chemical bonding interactions with the MB dye molecules, substantiating the chemisorption mechanism. Finally, the comparison with biomass-based adsorbents is presented in Table 5. In the present study, the adsorbent exhibited a maximum adsorption capacity of 454.54 mg/g.

Breakthrough time

Breakthrough time refers to the duration at which the concentration of the effluent reaches 60% of the initial influent concentration. The Box-Behnken design is useful for minimizing extreme experimental conditions, as it prevents all factors from being at their maximum or minimum values simultaneously. It is particularly effective when dealing with three levels of factors, which makes it an ideal choice for this experiment. The effect of process parameters of continuous adsorption was studied using response surface methodology based on Box-Behnken experimental design for the three factors at three levels using Minitab version 22.

Table 5 — Comparison of maximum adsorption capacity (q_m) of other biomass-based adsorbents reported for dye removal

Adsorbent	q_m(mg/g)	References
Pea Waste	167	26
V. cuspidata plant's leaves	35.7	62
Banana stalk waste	243.90	63
Quinoa waste biosorbents	193.8	64
Cassava bagasse	90.3	65
Terminalia catappa shells	88.62	66
Soybean hulls	169.9	67
Spent tea leaves	300.05	68
Waste Black Tea Powder	302.63	69
Tea waste	454.54	Present work

Effects of flow rate, bed height and bed diameter on breakthrough time

The contour interaction plot between flow rate (mL/min) and bed height (cm) on the breakthrough time is shown in Fig. 8. The darkest green area indicates maximum breakthrough time, suggesting

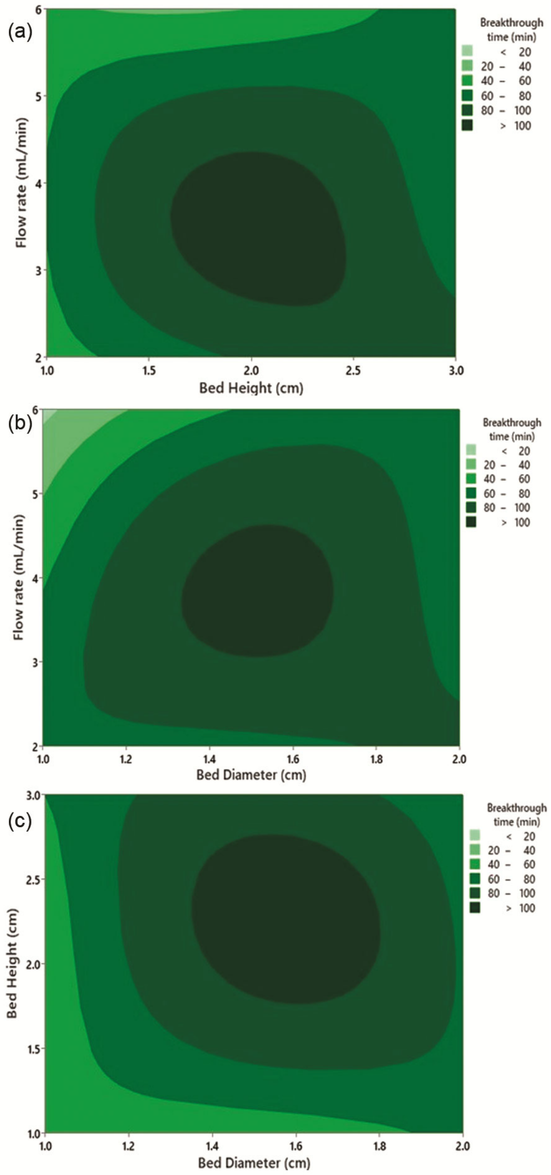

Fig. 8 — Contour interaction plot for the simultaneous effect of parameters (a) flow rate and bed height (b) flow rate and bed diameter and (c) bed height and bed diameter on breakthrough time

optimal conditions for longer operation before breakthrough occurs. Lower bed heights and higher flow rates show shorter breakthrough times, meaning the system becomes saturated more quickly. Increasing bed height generally improves performance (longer breakthrough time), but only up to a point beyond which the improvement may taper off.

The contour plot (Fig. 8b) illustrating the interaction between flow rate (mL/min) and bed diameter (cm) shows that the longest breakthrough time over 100 min is observed at the center of the plot, particularly around a flow rate of 4 mL/min and a bed diameter of 1.5 cm, which appears in the darkest green shade. As the flow rate increases, the breakthrough time tends to decrease, which is expected since a faster flow reduces the contact duration between the dye solution and the adsorbent, leading to earlier saturation. Similarly, reducing the bed diameter also slightly lowers the breakthrough time, especially when flow rates are high. The most favourable conditions for maximizing breakthrough time are found within the flow rate range of 3.5 to 4.5 mL/min and bed diameters between 1.4 and 1.6 cm.

As shown in Fig. 8(c), the contour interaction plot between bed height (cm) and bed diameter (cm) on the breakthrough time, in the center of the plot (around bed diameter of 1.6 cm and bed height of 2.2 cm) has the highest breakthrough time (darkest green, >100 min). It is the most optimal region for operation if the goal is to maximize breakthrough time. The lower left corner (bed diameter and height both close to 1.0 cm) shows the shortest breakthrough time (<20 min), meaning the system becomes saturated or ineffective much more quickly. As bed height increases, the fluid has a longer path through the adsorbent material, allowing more time for adsorption or filtration, thereby increasing breakthrough time. As bed diameter increases, the flow may become more evenly distributed, reducing channelling and improving usage of the bed, but to a lesser extent than height. There's a nonlinear interaction between bed height and diameter, as indicated by the curved contour lines. This suggests that increasing just one parameter does not always lead to proportional improvements; instead, an optimal combination of both gives the best results. Overall, high breakthrough times occur at low flow rates, large bed diameters, and large bed heights. This is due to the sufficient contact time between the dye and adsorbent at low flow rate and large adsorption site for the adsorption of dye on an adsorbent bed at large bed diameter and bed height.

Conclusion

Tea waste was successfully transformed into an efficient biosorbent for MB removal from water. SEM, FTIR, and XRD analyses confirmed MB adsorption on the tea waste surface and interior, showing clear morphological shifts and functional group changes, evidence of primarily physical adsorption. The Langmuir isotherm indicated monolayer adsorption with high capacity (q_{max} = 454.54 mg/g), confirming strong dye surface affinity. Adsorption kinetics followed a pseudo-second-order model (R^2 = 1.000), pointing to chemisorption involving electron exchange. Process optimization via Box–Behnken RSM yielded ideal conditions (4 mL/min flow, 2 cm bed height, 1.5 cm column diameter) with a 105 min breakthrough time, validating tea waste as a cost-effective and sustainable adsorbent for dye-laden wastewater treatment. Future work should focus on adsorbent regeneration, large-scale application, and extending use to other contaminants via material modification.

Acknowledgments

The authors are thankful to the Department of Chemical Engineering, Indian Institute of Technology Guwahati, Assam, India, for providing the research facilities.

Conflict of interest

The authors declare no conflict of interest.

References

1 Guo S, Kumar A M, Wang Y & Xu P, Current understanding in conversion and application of tea waste biomass: A review, *Bioresour Technol*, 338 (2021) 125530.

2 Dhongde N R, Das N K, Banerjee T & Rajaraman P V, Synthesis of carbon quantum dots from rice husk for anti-corrosive coating applications: Experimental and theoretical investigations, *Ind Crops Prod*, 212 (2024) 118329.

3 Seth D, Athparia M, Singh A, Rathore D, Venkatramanan V, Channashettar V, Prasad S, Maddirala S, Sevda S & Kataki R, Sustainable environmental practices of tea waste-A comprehensive review, *Environ Sci Pollut Res*, 32 (2023) 7449.

4 Dutta A, Kundu D, Naik P K, Silvester D S & Banerjee T, Synthesis and properties of physically cross-linked silica-mediated novel eutectogels developed from carboxylic acid-based natural deep eutectic solvents, *Ind Eng Chem Res*, 63 (2024) 18390.

5 Dutta A, Kundu D, Sharma S, Paul N, Naik P K, Silvester D S & Banerjee T, Physically cross-linked titania-supported

novel eutectogels as solid-state electrolytes: An experimental and quantum chemical investigation, *ACS Sustain Chem Eng*, 12 (2024) 248.

6 Alsarayreh A A, Al-zoubi H Q & Abbas M N, Sustainable nickel removal from water by using waste tea leaves for eco-friendly water treatment, *Indian Chem Eng*, (2025) 1.

7 Dhongde N R, Adhikari S & Rajaraman P V, Anticorrosion properties of ionic liquid functionalized graphene oxide epoxy composite coating on the carbon steel for CCUS environment, *Environ Sci Pollut Res*, (2025).

8 Dhongde N R, Baranwal P K & Rajaraman P V, Functionalization of graphene oxide with an ionic liquid (1-butyl-3-methylimidazolium acetate): Preparation of epoxy-based coating on carbon steel for anticorrosive applications, *J Appl Polym Sci*, 140 (2023).

9 Adhikari S, Dhongde N R, Talukdar M K, Khan S & Rajaraman P V, Investigation of carbon steels (API 5L X52 and API 5L X60) dissolution CO_2-H_2S solutions in the presence of acetic acid: Mechanistic reaction pathway and kinetics, *Arab J Sci Eng*, 49 (2024) 8363.

10 Dhongde N R, Das N K, Hazarika J, Park J G, Banerjee T & Rajaraman P V, Azoles as corrosion inhibitors in alkaline medium for ruthenium chemical mechanical planarization applications: Electrochemical and theoretical analysis, *J Mol Struct*, 1320 (2025) 139651.

11 Hussain S, Anjali K P, Hassan S T & Dwivedi P B, Waste tea as a novel adsorbent: A review, *Appl Water Sci*, 8 (2018) 165.

12 Subash A, Naebe M, Wang X & Kandasubramanian B, Tailoring electrospun nanocomposite fibers of polylactic acid for seamless methylene blue dye adsorption applications, *Environ Sci Pollut Res*, (2024).

13 Umesh A S, Puttaiahgowda Y M & Thottathil S, Enhanced adsorption: Reviewing the potential of reinforcing polymers and hydrogels with nanomaterials for methylene blue dye removal, *Surf Interf*, 51 (2024)104670.

14 Dhongde V, Velpandian M, Haider M A & Basu A, $Sr_2CoNbO_{6-\delta}$ @$Sm_{0.2}$ $Ce_{0.8}$ $O_{2-\delta}$ nanofiber composite as cathode accelerates oxygen reduction reaction for IT-SOFC, *ECS Trans*, 111 (2023) 2271.

15 Kusuma H S, Christa-Jaya D E, Illiyanasafa N, Ikawati K L, Kurniasari E, Darmokoesoemo H & Amenaghawon A N, A critical review and bibliometric analysis of methylene blue adsorption using leaves, *Chemosphere*, 356 (2024) 141867.

16 Doi A, Ganguly M & Sahu M, A comparative account on the elimination of methylene blue via iron-based nanoparticle: Adsorption vs. Degradation, *Adsorption*, 30 (2024) 1603.

17 Dutta A, Kundu D, Sharma S, Silvester D S & Banerjee T, Investigating the electrochemical properties of ionic-liquid-mediated inorganic eutectogels derived from carboxylic-acid-based hydrophobic natural deep eutectic solvents, *J Solution Chem*, (2025).

18 Dutta A, Millar W, Silvester D S & Banerjee T, Novel eutectogels derived from an ionic-liquid-based deep eutectic solvent as electrolytes for supercapacitors: Synthesis and characterization, *New J Chem*, 48 (2024)17787.

19 Ahsan M A, Katla S K, Islam M T, Hernandez-Viezcas J A, Martinez L M, Diaz-Moreno C A, Lopez J, Singamaneni S R, Banuelos J, Gardea-Torresdey J & Noveron J C, Adsorptive removal of methylene blue, tetracycline and Cr(VI) from water using sulfonated tea waste, *Environ Technol Innov*, 11 (2018) 23.

20 Borah L, Goswami M & Phukan P, Adsorption of methylene blue and eosin yellow using porous carbon prepared from tea waste: Adsorption equilibrium, kinetics and thermodynamics study, *J Environ Chem Eng*, 3 (2015) 1018.

21 Zhang Z, Abidi N & Lucia L, Smart superabsorbent alginate/carboxymethyl chitosan composite hydrogel beads as efficient biosorbents for methylene blue dye removal, *J Mater Sci Technol*, 159 (2023) 81.

22 Jayasuriya D M N H & Nadarajah K, Understanding association between methylene blue dye and biosorbent: Palmyrah sprout casing in adsorption process in aqueous phase, *Water Sci Eng*, 16 (2023) 154.

23 Grabi H, Ouakouak A, Kadouche S, Lemlikchi W, Derridj F & Din A T M, Mechanism and adsorptive performance of ash tree seeds as a novel biosorbent for the elimination of methylene blue dye from water media, *Surf Interf*, 30 (2022) 101947.

24 Pandey D, Daverey A, Dutta K, Yata V K & Arunachalam K, Valorization of waste pine needle biomass into biosorbents for the removal of methylene blue dye from water: Kinetics, equilibrium and thermodynamics study, *Environ Technol Innov*, 25 (2022) 102200.

25 Zein R, Purnomo J S, Ramadhani P, Safni, Alif M F & Putri C N, Enhancing sorption capacity of methylene blue dye using solid waste of lemongrass biosorbent by modification method, *Arab J Chem*, 16 (2023) 104480.

26 Holliday M C, Parsons D R & Zein S H, Agricultural pea waste as a low-cost pollutant biosorbent for methylene blue removal: adsorption kinetics, isotherm and thermodynamic studies, *Biomass Convers Biorefin*, 14 (2024) 6671.

27 Dominguez M, Mendoza J & Figueroa K, Adsorption of methylene blue dye using common walnut shell (*Juglans regia*) like biosorbent: Implications for wastewater treatment, *Green Chem Lett Rev*, 17 (2024) 2362257.

28 Praipipat P, Ngamsurach P, Srirat P & Chaiphumee P, Engineered biosorbents of pomelo (Citrus maxima (Burm.f.) Merr) peels modified with zinc oxide and titanium dioxide for methylene blue dye sorption, *Sci Rep*, 14 (2024) 5763.

29 Giahi M, Rakhshaee R & Bagherinia M A, Removal of methylene blue by tea wastages from the synthesis waste waters, *Chin Chem Lett*, 22 (2011) 225.

30 Uddin M T, Islam M A, Mahmud S & Rukanuzzaman M, Adsorptive removal of methylene blue by tea waste, *J Hazard Mater*, 164 (2009) 53.

31 Ullah A, Zahoor M, Din W U, Muhammad M, Khan F A, Sohail A, Ullah R, Ali E A & Murthy H C A, Removal of methylene blue from aqueous solution using black tea wastes: Used as efficient adsorbent, *Adsorpt Sci Technol*, 2022 (2022).

32 El-Azazy M, El-Shafie A S & Al-Shaikh Y B, Green tea waste as an efficient adsorbent for methylene blue: Structuring of a novel adsorbent using full factorial design, *Molecules*, 26 (2021) 6138.

33 Jain D M & Singh V, Experimental and modelling study of industrial phenolic wastewater treatment by packed bed adsorption on coal-based and bagasse-based fly ash, *Indian Chem Eng*, 64 (2022) 171.

34 Meshram S, Dharmadhikari S, Thakur R S, Soni A B & Thakur C, Fixed-bed adsorption of lead from battery recycling unit wastewater-optimization using Box-Behnken method, *J Hazard Mater Adv*, 10 (2023) 100297.

35 Hiremath P G, Rajashekhara S, Sarkar S, Kumar H S & Thejashree V, Treatment of fluoride-contaminated water in a prototype adsorption unit using zirconium-activated carbon nanocomposites, *Indian Chem Eng*, (2024) 1.

36 Thalya P P, Sinha S, Sainath K & Siddiqui S, Computational intelligence modelling of methylene blue adsorption by metal-organic frameworks, *Indian Chem Eng*, 66 (2024) 349.

37 Mussa Z H, Al-Ameer L R, Al-Qaim F F, Deyab I F, Kamyab H & Chelliapan S, A comprehensive review on adsorption of methylene blue dye using leaf waste as a bio-sorbent: Isotherm adsorption, kinetics, and thermodynamics studies, *Environ Monit Assess*, 195 (2023) 940.

38 Malhotra M, Suresh S & Garg A, Tea waste derived activated carbon for the adsorption of sodium diclofenac from wastewater: Adsorbent characteristics, adsorption isotherms, kinetics, and thermodynamics, *Environ Sci Pollut Res*, 25 (2018) 32210.

39 Meena P L, Saini J K, Surela A K, Poswal K & Chhachhia L K, Fabrication of polyaniline-coated porous and fibrous nanocomposite with granular morphology using tea waste carbon for effective removal of rhodamine B dye from water samples, *Biomass Convers Biorefin*, 14 (2024) 1711.

40 Meshram S, Thakur R S, Jyoti G, Thakur C & Soni A B, Optimization of lead adsorption from lead-acid battery recycling unit wastewater using H_2SO_4 modified activated carbon, *J Indian Chem Soc*, 99 (2022) 100469.

41 Meshram S, Dhongde N R, Pandey L, Dewangan G P & Joshi A N, Efficacy of hazardous congo red removal from aqueous solutions via adsorption with carbon black: Batch and column study insights, *Indian J Chem Technol*, 32 (2025) 572.

42 Borah M, Konwar U, Gogoi P, Boruah P, Bora J G, Garg S, Ahmed T H & Das B, Decolorization of tea industry wastewater utilizing tea waste bio-adsorbent in fixed-bed adsorption column: Breakthrough curves analysis and modelling, *Sustain Water Resour Manag*, 10 (2024) 37.

43 Singh J, Kumar A, Pathak A & Palai T, Adsorptive removal of arsenic(III) from contaminated water using rice husk, tea waste and sugarcane bagasse bio-adsorbents, *Water Air Soil Pollut*, 234 (2023) 308.

44 Guven M, Isik B, Cakar F & Cankurtaran O, Removal of toxic methylene blue dye from aqueous solutions by adsorption technique using magnetic loaded tea waste and its sodium alginate composite microspheres, *Environ Monit Assess*, 197 (2025) 664.

45 Kızıltaş H, Production of highly effective adsorbent from tea waste, and its adsorption behaviors and characteristics for the removal of Rhodamine B, *Int J Environ Anal Chem*, 104 (2024) 1730.

46 Bala K, Sharma D, Kumar N, Gupta N & Raja V, Tea waste-derived charcoal as an efficient adsorbent for the removal of rhodamine B, *Biomass Convers Biorefin*, 14 (2024) 25837.

47 Ateş A, Mert Y & Timko M T, Evaluation of characteristics of raw tea waste-derived adsorbents for removal of metals from aqueous medium, *Biomass Convers Biorefin*, 13 (2023) 7811.

48 Hasan M, Al-Biruni M T, Azad S & Ahmed T, Adsorptive removal of dye from textile wastewater employing Moringa oleifera leaves biochar as a natural biosorbent, *Biomass Convers Biorefin*, 14 (2024) 11075.

49 Sharma S, Hasan A, Kumar N & Pandey L M, Removal of methylene blue dye from aqueous solution using immobilized Agrobacterium fabrum biomass along with iron oxide nanoparticles as biosorbentm, *Environ Sci Pollut Res*, 25 (2018) 21605.

50 Zein R, Satrio-Purnomo J, Ramadhani P, Safni, Alif M F & Putri C N, Enhancing sorption capacity of methylene blue dye using solid waste of lemongrass biosorbent by modification method, *Arab J Chem*, 16 (2023) 104480.

51 Rajput M K, Hazarika R & Sarma D, Zerovalent iron decorated tea waste derived porous biochar [ZVI@TBC] as an efficient adsorbent for Cd(II) and Cr(VI) removal, *J Environ Chem Eng*, 11 (2023) 110279.

52 Mariah M A A, Rovina K, Vonnie J M & Erna K H, Characterization of activated carbon from waste tea (Camellia sinensis) using chemical activation for removal of methylene blue and cadmium ions, *S Afr J Chem Eng*, 44 (2023) 113.

53 Zhang N, Reguyal F, Praneeth S & Sarmah A K, A green approach of biochar-supported magnetic nanocomposites from white tea waste: Production, characterization and plausible synthesis mechanisms, *Sci Total Environ*, 886 (2023) 163923.

54 Wu J, Annath H, Chen H & Mangwandi C, Upcycling tea waste particles into magnetic adsorbent materials for removal of Cr(VI) from aqueous solutions, *Particuology*, 80 (2023) 115.

55 Khurshid H, Mustafa M R U, Rashid U, Isa M H, Ho Y C & Shah M M, Adsorptive removal of COD from produced water using tea waste biochar, *Environ Technol Innov*, 23 (2021) 101563.

56 Meshram S, Thakur C & Soni A B, Adsorption of Pb(II) form battery recycling unit effluent using granular activated carbon (GAC) and steam activated GAC, *Indian Chem Eng*, 63 (2021) 460.

57 Meshram S, Joshi A N, Dharmadhikari S & Thakur R S, Adsorption of cadmium from water using activated carbon derived from ipomoea carnea using chemical impregnation, *IOP Conf Ser Earth Environ Sci*, 597 (2020) 012005.

58 Meshram S, Thakur R S, Jyoti G, Thakur C & Soni A B, Optimization of lead adsorption from lead-acid battery recycling unit wastewater using H_2SO_4 modified activated carbon, *J Indian Chem Soc*, 99 (2022) 100469.

59 Koujalagi P S, Divekar S V, Kulkarni R M & Cuerda-Correa E M, Sorption of hexavalent chromium from water and water-organic solvents onto an ion exchanger Tulsion A-23(Gel), *Desal Water Treat*, 57 (2016) 23965.

60 Meshram S, Thakur C & Soni A, Fixed bed adsorption treatment of effluent of battery recycling unit to remove Pb(II) using steam-activated granular carbon, *J Serb Chem Soc*, 85 (2020) 953.

61 Ho Y S & McKay G, Pseudo-second order model for sorption processes, *Process Biochemistry*, 34 (1999) 451.

62 Awad H E A, Mohammad A M & Farahat E A, Potential use of dry powder of Vossiacuspidata (Roxb.) Griff. rhizomes and leaves in methylene blue dye remediation, *Sci Rep*, 13 (2023) 11073.

63 Hameed B H, Mahmoud D K & Ahmad A L, Sorption equilibrium and kinetics of basic dye from aqueous solution using banana stalk waste, *J Hazard Mater*, 158 (2008) 499.

64 Oulkhir A, Lyamlouli K, Danouche M & Benhida R, Biosorption of a cationic dye using raw and functionalized

Chenopodium quinoa pericarp biomass after saponin glycosides extraction, *J Environ Chem Eng*, 11 (2023) 110419.

65 Diehl M, Silva L F O, Schnorr C, Netto M S, Bruckmann F S & Dotto G L, Cassava bagasse as an alternative biosorbent to uptake methylene blue environmental pollutant from water, *Environ Sci Pollut Res*, 30 (2023) 51920.

66 Hevira L, Zilfa, Rahmayeni, Ighalo J O, Aziz H & Zein R, Terminalia catappa shell as low-cost biosorbent for the removal of methylene blue from aqueous solutions, *J Ind Eng Chem*, 97 (2021) 188.

67 Cusioli L F, Quesada H B, Baptista A T A, Gomes R G & Bergamasco R, Soybean hulls as a low-cost biosorbent for removal of methylene blue contaminant, *Environ Prog Sustain Energy*, 39 (2020) e13328.

68 Hameed B H, Spent tea leaves: A new non-conventional and low-cost adsorbent for removal of basic dye from aqueous solutions, *J Hazard Mater*, 161 (2009) 753.

69 Lin D, Wu F, Hu Y, Zhang T, Liu C, Hu Q, Hu Y, Xue Z, Han H & Ko T H, Adsorption of dye by waste black tea powder: Parameters, kinetic, equilibrium, and thermodynamic studies, *J Chem*, 2020 (2020) 1.